

Automatic Recognition of Bio-Colonization Processes on Historic Facades: Application on Case Studies

Francesco Monni^{1*}, Marco D'Orazio¹, Andrea Gianangeli¹, Enrico Quagliarini¹.

1 - Dipartimento di Ingegneria Civile, Edile e Architettura (DICEA) - Università Politecnica delle Marche, Ancona, Italy

* f.monni@univpm.it

Abstract

Many factors (physical, chemical, natural, and human activities) contribute to the degradation of historic buildings. Preventive conservation is a cost-effective approach international preservation bodies recommend to mitigate risks to built cultural heritage. A substantial challenge is bio-colonization, especially by microalgae, which affects brick-facing masonry surfaces due to environmental factors (i.e., temperature and moisture), leading to progressively increasing deterioration. Early detection systems could be useful to reduce damage from these organisms. Advances in computer vision and machine learning, such as convolutional neural networks, offer promising solutions for automating the identification of building pathologies using image collection. This research focuses on developing predictive models using convolutional neural networks to monitor bio-deterioration on historic facades, specifically targeting early-stage microalgae colonization. After a training phase using laboratory-induced bio-colonization on brick samples, the method was applied to real case studies of architecturally significant buildings affected by bio-colonization. In fact, a substantial number of digital images of these buildings, even if taken for other purposes, are available. The work shows that analyzing these images with the trained network facilitates the early detection of bio-colonization, providing a contribution to the field of built cultural heritage conservation.

Keywords: Microalgae, Bio-colonization, Historical buildings, Convolutional neural network, Monitoring

1. Introduction

The deterioration of historic building heritage is driven by a combination of physical, chemical, natural, and human-induced factors [1]. It is recognized that preventive conservation is one of the most cost-effective approaches, also recommended by international institutions involved in preservation [2], and consists of «a set of actions useful for reducing risk situations concerning cultural assets in their context» [3]. Bio-colonization (growth of living microorganisms) is one of the several pathologies affecting historical heritage that should be paid attention to. Historical buildings could be affected by primary (microalgae), secondary (molds and lichens), or tertiary (plants) colonizers, and the restoration of the affected surfaces can be costly. The colonization process by microalgae (primary colonizers) starts from an interaction between environmental factors and the physical and chemical properties of clay brick [4]. In the case of buildings of cultural value, the growth of these organisms could cause severe losses in original materials [5]. Adequate temperature and availability of water can indulge the growth of microalgae and, therefore, the degradation of the material, contributing to the creation of a suitable environment for the growth of other colonizers [4][6][7].

Furthermore, porosity and roughness of the substrate can promote algae growth [8][9]. In this context, the availability of early detection systems based on data collection and images can help limit the aesthetic, chemical, and physical

43 degradation of building surfaces due to bio-colonizers. The topic of computer vision-based automated building
44 pathologies identification (using image processing and machine learning techniques) has attracted research attention in
45 recent years, particularly about crack detection [10] on concrete [11] and masonry structures [12]. A convolutional
46 neural network is a specialized type of deep learning model designed to process and analyze structured grid-like data,
47 such as images. It is particularly effective in tasks involving image recognition and classification because it can
48 automatically learn spatial hierarchies of features through convolutional layers. In the field of architectural heritage,
49 convolutional neural network classification techniques have been used to identify and locate several types of damage
50 (i.e., stain, efflorescence, cracks, and spalling) in masonry buildings [13][14]. The issue of bio-colonizers on existing
51 buildings has been addressed in [15] about tertiary colonizers (plants).

52 Regarding the specific problem of microalgae, in literature, there are available works focused on digital images
53 acquired during the growth of microalgae strains in water solution but not on building facades [16]. In this work, to fill
54 the lack of existing literature, the development of predictive models using a convolutional neural network useful to
55 automatically monitor the bio-deterioration status of historic building heritage with facing masonry facades is
56 proposed. Given that digital images of historical building facades are constantly being captured and collected for
57 various purposes (e.g., photographic documentation and tourist information), as well as automatically provided by
58 surveillance cameras, there is a substantial amount of material available to assess the condition of these surfaces using
59 the proposed method. The findings of this work serve as a preliminary step toward developing tools for the early
60 detection of damage to building facades, particularly biodeterioration.

61 **2. Methodology**

62 *2.1 Research framework*

63 To reach the proposed goal, the research process was set up as follows: first, an experimental activity has been
64 developed to follow, in controlled conditions, the microalgae growth, considering diverse types of clay bricks and
65 various exposure conditions (temperature, RH%, rain). Then, digital images collected during the experimental
66 campaign were resized and cropped to generate a dataset of about 12.000 sub-images representing the various stages
67 of the bio-deterioration process. A convolutional neural network was trained using the digital images dataset that was
68 obtained. Finally, the method was tested on case studies with brick-facing masonry to verify its applicability as an early
69 detection system.

70 *2.2 Experimental campaign*

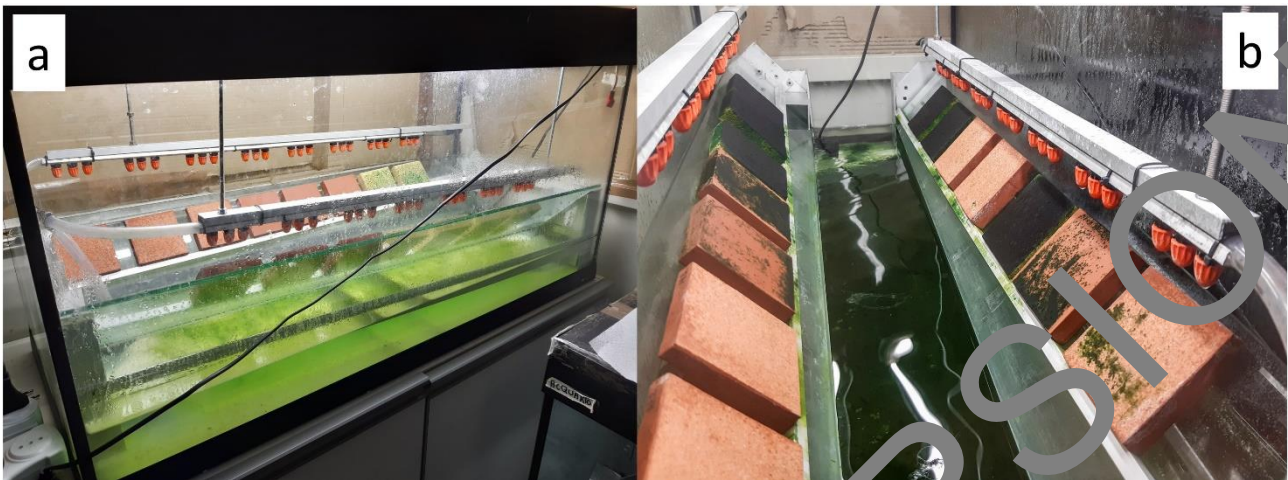
71 The digital images to be used to train the convolutional neural network were obtained from an experimental
72 campaign in which five types of clay bricks (designated as AH, AL, B, CH, and CL) were selected and tested in five
73 different environmental conditions, reproduced using climatic chambers to accelerate the growth process. Clay bricks
74 differ by color, porosity, and roughness. Considering that bio-colonization causes a shift of the original color towards
75 green-blue nuances, and the initial color spectrum is influenced due to the transition between wetted and unwetted
76 conditions, were chosen three different brick colors: light-red (AH and AL types), dark-red (B type), yellow (CH and
77 CL types). Because the “shape” of the bio-colonization (e.g., spots, lines, areas) is influenced by the surface features
78 and the water retention characteristic of the clay bricks, different microstructures were considered. Different
79 environmental conditions were considered and characterized by different temperatures, RH%, and wetting processes to

80 include a wide range of expected environmental conditions. Surface properties like porosity (according to ASTM
81 D4404-10 [17]) and roughness (according to UNI EN ISO 4287:2009 [18]) of the tested clay bricks were measured. A
82 green alga (*Chlorella mirabilis* strain ALCP 221B) and a cyanobacterium (*Chroococcidiopsis fissurarum* strain IPPAS
83 B445) were used to reproduce the bio-colonization process [7]. Microbial strains were cultivated in a Bold's Basal
84 Medium (BBM), formulated following ASTM D5589-09 prescriptions [19]. To reduce testing times, the tests were
85 conducted under accelerated conditions (a visible biological degradation mostly begins after at least one year of natural
86 environmental exposure). Five distinct environmental conditions were chosen to take into account a wide variety of
87 potential real exposures. To find out how changing relative humidity (RH) levels affected algae growth on clay brick
88 surfaces, three distinct RH conditions were replicated in three different climatic chambers.

89 Saturated solutions were used to condition the indoor environment, as recommended by EN ISO 12571:2013 [20]. The
90 first RH condition (RH1, around 75%) was obtained using a saturated solution of NaCl; the second RH condition (RH2,
91 around 87%) was obtained using a saturated solution of Na₂CO₃; the third RH condition (RH3, around 98%) was obtained
92 using only deionized water. Tests were conducted at constant temperature (27.5 ± 2.5 °C) in order to examine the impact
93 of RH only. Each sample had nine distinct locations on its surface that were inoculated with 5µL of the mixed culture at
94 the start of the test. After that, samples were placed, with an inclination of 45° on aluminum-glass racks inside the
95 climatic chambers, front-to-front along the chamber's long length. In order to protect the test equipment from outside
96 influences such as light, temperature, and relative humidity, it was housed in a closed room. Two neon lights (Sylvania
97 TopLife 39W) able to faithfully reproduce natural light conditions were installed in each growth chamber with the aim
98 of recreating day/night cycles 14/10 h (Figure 1a). The impact of temperature on algae growth was investigated in the
99 wake of previous studies available in the literature [8][9]. Until the stagnation phase was reached, accelerated tests were
100 conducted using periodic water sprays on the material's surface (Figure 1b). Growth chambers (100×40×53 cm³)
101 containing 35 liters of BBM inoculated with the mixed cultures represent the test apparatus for this phase of the work.
102 Algal suspension was applied (sprayed) to sample surfaces (8×8 cm²) situated on two 45°-inclined racks made of
103 aluminum and glass. Run/off cycles were programmed to occur every 15 minutes for a total of 6 hours a day (3 hours of
104 run time and 3 hours of rest time). Two 39W neon lights (Sylvania TopLife) have been used to reproduce a day/night
105 lighting cycle of 14/10 hours. Following existing literature [21][22], two distinct temperatures were chosen for the
106 accelerated tests: 27.5 ± 2.5 °C, which falls within the range of ideal growth values (which span from 20 °C to 30 °C),
107 and a lower value of 10 ± 2.5 °C, which falls within the range of suitable growth. A properly modified refrigerator
108 (Electrolux RC 520 A DW2) was utilized to set the lower test temperature. The presence of the wetting cycles makes it
109 reasonable to assume that the relative humidity was always 100%. Temperature and relative humidity sensors (Sensirion
110 SHT31-B) were used to monitor all test settings, with data taken every 10 minutes. During each accelerated growth test,
111 specific analyses were performed to evaluate the algal extent and the biofouling process on the samples' surface [8].
112 First, colorimetric analysis was done to check how the color changed over time. A spectrophotometer (Konika Minolta
113 CM-200dD) was used to quantify the chromatic variation (ΔE) [17]. According to UNI EN 15886:2010 [23] and UNI
114 11721:2018 [24], the CIELAB color space was used to represent the results. Equation (1) was used to determine color
115 variation in terms of total color difference (ΔE)

$$\Delta E = \sqrt{(L_0^* - L^*)^2 + (a_0^* - a^*)^2 + (b_0^* - b^*)^2} \quad (1)$$

120 where L^* , a_0^* , b_0^* are the color coordinates of samples before the test (time zero), and L^* , a^* , b^* are those evaluated during
121 the accelerated growth phase. The value has been measured on nine different spots on each sample surface every week.
122



123
124 Figure 1 – The test setup used to evaluate the effects of relative humidity on microalgae growth development (a) and the
125 one used to investigate the impact of temperature (b).

126 2.3 Digital image acquisition and division

127 A high-resolution scanner (HP Scanjet G3010) was used weekly to collect digital images to train the convolutional
128 neural network. Previous works [8] have proven the effectiveness of this technique. As mentioned in the following part,
129 the obtained images were elaborated using “ImageMagick” software. The “Imagemagick” software (rel.7.1.1-20) allowed
130 the scaling of the images to 1780x1780 pixels; these were then cropped to create 256x256 sub-images: 49 sub-images were
131 produced from each image. The name and order of every sub-image were changed randomly, and after that, a manual
132 annotation procedure was carried out. Matlab software (rel. 2023a) was used to filter the image’s R, G, and B channels in
133 order to make the annotation process easier and take into account the fact that microalgae growth results in a color shift
134 towards green values. Images with microalgae presence traces were labeled as “algae”, while the others were labeled as
135 “no_algae”. Finally, the 13.12 sub-images that composed the annotated picture dataset were split equally into two
136 sections: “train” and “test”. There were 1780 “no_algae” and 4780 “algae” photos in each dataset segment. No filtering
137 was applied to the output images to evaluate the trained and tested convolutional neural network’s capacity to operate
138 directly with real pictures [25].

139 2.4 Convolutional neural network design and training

140 A convolutional neural network is called a feed-forward neural network with many convolutional layers layered on top
141 of one another, each one able to recognize increasingly complex forms. Pooling layers (subsampling layers) are included.
142 By calculating a summary statistic from the outputs in the vicinity, the pooling layer substitutes the network’s output at
143 specific points. This reduces the spatial dimensions of the representation, which in turn decreases the amount of
144 computation required and leads to more efficient and faster model performance. Following a hyper-tuning procedure, a
145 two-convolution layer was selected to maximize the convolutional neural network’s layer count. The first convolutional
146 layer has dimension [32, (3,3)]. The second convolutional layer has the dimension [64, (3,3)]. In order to turn the final
147 matrix into a single array, two pooling layers, two dense layers (256,1), and a flatten layer were added. The first dense
148 layer and the second convolutional layers use the “Relu” activation function. The second “dense” layer has been designated

149 for the “Sigmoid” activation function. RMSprop optimizer (learning rate = 0.001) has been considered. The accuracy
150 measure was displayed because our challenge is binary classification. The ratio of accurate forecasts to total predictions
151 made by the model is known as accuracy. For the training procedure, batch sizes of 20 and 50 epochs were considered.
152 The convolutional neural network has been trained and tested using a Python script (rel 3.9). The convolutional neural
153 network was trained and tested using the “Tensorflow” and “Keras” libraries; then, it was hyper-tuned (parameter
154 optimized) using the “Keras-tuner” library.

155 2.5 Application to case studies

156 Two specific case studies have been selected to demonstrate the practical applicability of the proposed model: the “Mole
157 Vanvitelliana” and the “Rocca Roveresca”, two historical buildings of high architectural value that exhibit evident bio-
158 colonization problems.

159 The “Mole Vanvitelliana” (Figure 2) is a large, pentagonal architectural complex from the 16th century, located by the sea
160 in the port area of Ancona (Marche region, Italy). This structure, also known as the “Pizzaretto,” originally served as a
161 quarantine station for those arriving by sea in Ancona (a precautionary measure to monitor and control the spread of
162 contagious diseases). Over the years, the building has been repurposed for various uses, including military and commercial
163 functions, and today, it operates as a multifunctional cultural center. Designed in the 16th century by the architect Luigi
164 Vanvitelli, the “Mole Vanvitelliana” is a unique example of architecture and a notable symbol of the city of Ancona. The
165 main building of the complex is enclosed within a perimeter wall. Both the primary structure and the surrounding wall are
166 constructed with brick-facing masonry. Notably, the sloped, rain-exposed perimeter walls show significant signs of bio-
167 colonization, whereas the vertical walls of the main building, which are sheltered from the rain, do not exhibit such issues.
168



169
170 Figure 2 – The Mole Vanvitelliana – Ancona – Marche Region - Italy
171

172 The “Rocca di Senigallia”, also known as “Rocca Roveresca” after the Della Rovere family who commissioned its
173 construction (Figure 3), is located in Senigallia (Marche region, Italy), and it stands as one of the most significant
174 monuments of both the city and the region. As it appears today, the fortress is the result of centuries of transformation.
175 Originally built during the Roman era as a defensive tower, it evolved into a medieval fortress in the 14th century and
176 eventually took its current form as a typical Renaissance fortified residence in the 15th century. The monument consists of
177 two interconnected structures: the central body, intended as a noble residence, is surrounded by a military defensive
178 structure. The noble residence is encircled by a highly regular structure: a quadrilateral enclosure with four low circular

179 towers at the corners, all connected to each other and the central building by an integrated system of vertical and horizontal
180 communication routes. As in the previous case, the perimeter walls are made of brick-facing masonry. As shown in the
181 figure, some portions of the structure, particularly those with a sloped configuration that makes them more exposed to
182 weather conditions, exhibit signs of bio-colonization (specifically, the lower parts of the perimeter walls). In contrast, other
183 areas are more protected and do not suffer from this issue.
184



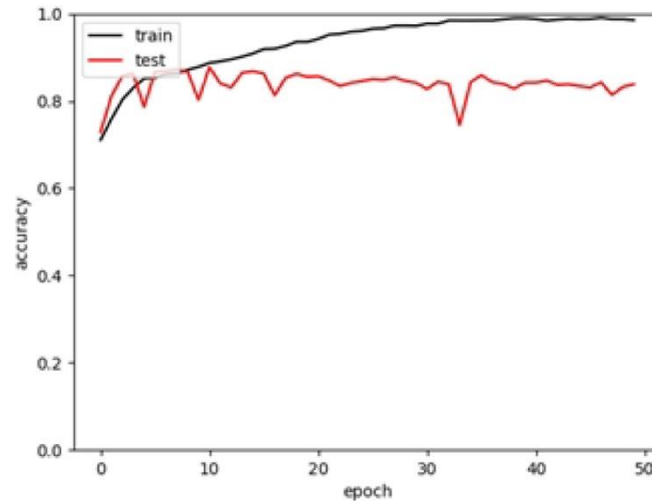
185
186 Figure 3 – The Rocca Roveresca – Senigallia – Marche Region – Italy
187

188 Two different datasets of images were collected from the two case studies. Firstly, digital images extracted from video
189 surveillance HD cameras were collected to evaluate the model's applicability to this type of data source. The second dataset
190 consisted of images of brick-facing masonry facades captured manually using an HQ resolution camera. All the images
191 were resized to the same dimension (1780x1780) using the "ImageMagick" tool, rel.7.1.1-20, and cropped to obtain ca.
192 1550 256x256 pixels sub-images coming from video surveillance cameras and ca. 500 sub-images of 256x256 pixels from
193 the HQ resolution camera images.

194 3. Results

195 3.1 Convolutional neural network training and test

196 A trained, tested, and validated convolutional neural network has been used to determine the beginnings of the microalgae
197 development process. The plot of the historical training and test procedure is displayed in Figure 4. The accuracy using the
198 "training" and "test" datasets has been displayed after each epoch (iteration on the whole dataset). When the final accuracy
199 or the ratio of accurate predictions to all predictions produced by the model is 0.83, meaning that 83% of the photos,
200 which they included microalgae or not, were identified correctly.
201



202

203 Figure 4 - Plot of the “training and test” history process. The black line represents the accuracy obtained at the end of
204 each epoch during the training process. The red line represents the accuracy obtained at the end of each epoch during the
205 test process.

206 *3.2 Automatic detection of bio-colonization on case studies*

207 The trained model was applied iteratively to verify its recognition ability in real cases. The trained network was first used
208 to detect bio-colonization presence in images collected by security IP cameras. The application of the method to this
209 group of images highlighted that the ability to recognize bio-colonization on the brick-facing masonry facades is affected
210 by several factors. Dividing images from surveillance cameras results in low-resolution sub-images, reducing recognition
211 effectiveness. Moreover, images acquired from security cameras include other elements (ground, grass, roads, roofs, stone,
212 metallic elements, etc.) that were not included in the original dataset. If the cropped image contains objects different from
213 the bricks, convolutional neural networks frequently fail, reducing total accuracy to unacceptable values. This clearly
214 highlights two things. First, there is a need for higher resolution images, and second, there is a necessity to expand the
215 dataset used to train the convolutional neural networks by including images of the brick surface and images featuring all
216 elements present on and around building facades (Figure 5).

217



218

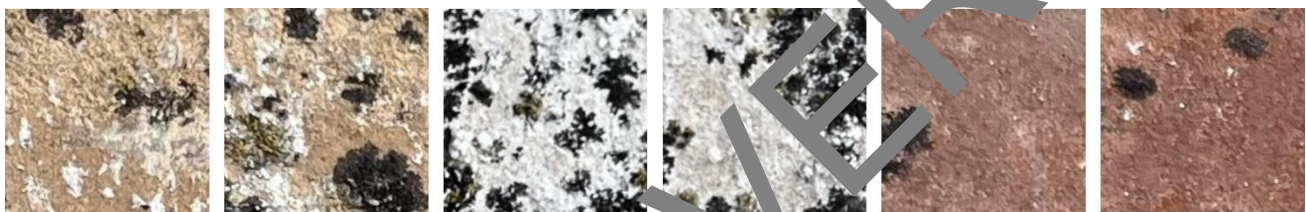
219 Figure 5 – Some examples of images extracted from HD security cameras installed at the Mole Vanvitelliana and the
220 Rocca Roveresca.

221
222 Then, the trained network was used to detect bio-colonization presence in the second group of images, those directly
223 collected near the building facades, which include only bricks with and without bio-colonization (Figure 6). In this scenario,
224 accuracy improves to 0.68 but remains below the one achieved after the training and testing phases (0.83). Thus, enhancing
225 resolution and excluding non-brick elements improved the recognition performance of the trained convolutional neural
226 networks.

227 However, the not-perfect matching among the colors of the bricks used to train the convolutional neural networks and the
228 color of the historical clay bricks of the case studies, along with the potential presence of other types of bio-colonizers
229 and/or stains, reduced the accuracy achieved with real images.

230 It is important to note that no image filtering was conducted to evaluate the performance of the trained and tested
231 convolutional neural networks to work directly with real images.

232



233

234 Figure 6 – Some examples of images collected with HQ resolution cameras at the Mole Vanvitelliana and the Rocca
235 Roveresca

236 4. Conclusions

237 Architectural heritage is subjected to many deterioration problems; one of these is the phenomenon of biodeterioration and,
238 in particular, microalgae growth. Following the preventive conservation approach, this work aims to provide a tool for
239 “early” damage detection in order to reduce major invasive interventions, moving from restoration (intended as those
240 activities needed to repair serious deteriorations) to a more inclusive approach based on continuous care and supported by
241 data collection, regular monitoring, inspections, control of environmental factors and maintenance activities. In this
242 context, predictive models based on convolutional neural networks that can detect microalgae growth on facing-masonry
243 surfaces were studied and developed. The convolutional neural network has been trained with images collected during an
244 experimental campaign. The model obtained after the training phase is able to recognize the beginnings of the bio-
245 colonization process on several types of clay bricks and can rely on an accuracy of 83%. The initial results from applying
246 the described procedure to a case study were promising but nonetheless highlighted some issues. While automatically
247 obtained images from surveillance systems proved less effective (due to their low quality and the inclusion of contextual
248 elements that interfere with the recognition system), using high-quality images, even those taken for other purposes, yielded
249 significantly better outcomes. However, the application to case studies has not yet achieved results comparable to those
250 obtained in laboratory samples, indicating that further refinement is still needed. To address the primary limitation
251 identified, it will be necessary to extend this study by expanding the dataset through additional experimental activities and
252 incorporating real-world images that capture all elements found on building facades and their surroundings, as well as
253 images of various types of bio-colonizers, into the training process.

254 5. Funding

255 ~~This research has received funding from the project Vitality—Project Code ECS00000041, CUP I33C22001330007~~
256 ~~—Call for tender No. 3277 of 30/12/2021, and Concession Decree No. 0001057.23-06-2022 of Italian Ministry of~~
257 ~~University funded by the European Union—NextGenerationEU.~~

258 This research has received funding from the project Vitality – Project Code ECS00000041, CUP I33C22001330007
259 - funded under the National Recovery and Resilience Plan (NRRP), Mission 4 Component 2 Investment 1.5 - 'Creation
260 and strengthening of innovation ecosystems,' construction of 'territorial leaders in R&D' – Innovation ecosystems -
261 Project 'Innovation, digitalization and sustainability for the diffused economy in Central Italy – VITALITY' Call for
262 tender No. 3277 of 30/12/2021, and Concession Decree No. 0001057.23-06-2022 of Italian Ministry of University
263 funded by the European Union – NextGenerationEU.

264 6. Author Contributions

265 The paper was elaborated as a team, but M.D. designed and directed the project and developed the neural network;
266 A.G. and E.Q. designed and performed the experimental phases, and F.M. contributed to data collection and case-study-
267 related activities. Writing – Original Draft and Writing – Review & Editing are realized by the authors unless otherwise
268 specified.

269 7. References

- 270 [1] E. Eken, B. Taşçı, and C. Gustafsson, “An evaluation of decision-making process on maintenance of built
271 cultural heritage: The case of Visby, Sweden,” *Cities*, vol. 94, pp. 24–32, 2019, doi: 10.1016/j.cities.2019.05.030.
- 272 [2] ICOMOS, “ICOMOS Charter – Principles for the Analysis, Conservation and Structural Restoration of Heritage,
273 Architectural.” 2003. [Online]. Available: [http://www.icomos.org/en/about-the-centre/179-articles-en-](http://www.icomos.org/en/about-the-centre/179-articles-en-francais/ressources/charters-and-standards/155-icomos-charter-principles-for-the-analysis-conservation-and-structural-restoration-of-architectural-heritage)
274 [francais/ressources/charters-and-standards/155-icomos-charter-principles-for-the-analysis-conservation-and-](http://www.icomos.org/en/about-the-centre/179-articles-en-francais/ressources/charters-and-standards/155-icomos-charter-principles-for-the-analysis-conservation-and-structural-restoration-of-architectural-heritage)
275 [structural-restoration-of-architectural-heritage](http://www.icomos.org/en/about-the-centre/179-articles-en-francais/ressources/charters-and-standards/155-icomos-charter-principles-for-the-analysis-conservation-and-structural-restoration-of-architectural-heritage)
- 276 [3] J. Sroczynska, “Preventive maintenance of historical buildings in European countries,” vol. 2, no. 70, pp. 51–57,
277 2022, doi: 10.37191/arc22.005.
- 278 [4] G. Canevali, M. P. Nigari, O. Salvadori, and ICCROM - International Centre for the Study of the Preservation and
279 the Restoration of Cultural Property, *Biology in the Conservation of Works of Art*. Roma: Sintesi Grafica Srl,
280 1991.
- 281 [5] R. De la Cruz-Jones, J. J. Hughes, S. Jones, and T. Yarrow, “Science, value and material decay in the conservation
282 of historic environments,” *J. Cult. Herit.*, vol. 21, pp. 823–833, 2016, doi: 10.1016/j.culher.2016.03.007.
- 283 [6] T. Warscheid and J. Braams, “Biodeterioration of stone: A review,” *Int. Biodeterior. Biodegrad.*, vol. 46, no. 4,
284 343–368, 2000, doi: 10.1016/S0964-8305(00)00109-8.
- 285 [7] L. Tomaselli, G. Lamenti, M. Bosco, and P. Tiano, “Biodiversity of photosynthetic microorganisms dwelling on
286 stone monuments,” *Int. Biodeterior. Biodegrad.*, vol. 46, no. 3, pp. 251–258, 2000, doi: 10.1016/S0964-
287 8305(00)00078-0.
- 288 [8] L. Graziani, E. Quagliarini, A. Osimani, L. Aquilanti, F. Clementi, and M. D’Orazio, “The influence of clay
289 brick substratum on the inhibitory efficiency of TiO₂ nanocoating against biofouling,” *Build. Environ.*, vol. 82,
290 pp. 128–134, Dec. 2014, doi: 10.1016/j.buildenv.2014.08.013.

- 291 [9] L. Graziani, E. Quagliarini, and M. D’Orazio, “The role of roughness and porosity on the self-cleaning and anti-
292 biofouling efficiency of TiO₂ Cu and TiO₂ Ag nanocoatings applied on fired bricks,” *Constr. Build. Mater.*, vol.
293 129, pp. 116–124, 2016, doi: 10.1016/j.conbuildmat.2016.10.111.
- 294 [10] H. S. Munawar, A. W. A. Hammad, A. Haddad, C. A. P. Soares, and S. T. Waller, “Image-based crack detection
295 methods: A review,” *Infrastructures*, vol. 6, no. 8. MDPI AG, Aug. 01, 2021. doi:
296 10.3390/infrastructures6080115.
- 297 [11] B. Kim and S. Cho, “Automated vision-based detection of cracks on concrete surfaces using a deep learning
298 technique,” *Sensors (Switzerland)*, vol. 18, no. 10, Oct. 2018, doi: 10.3390/s18103452.
- 299 [12] D. Loverdos and V. Sarhosis, “Automatic image-based brick segmentation and crack detection on masonry walls
300 using machine learning,” *Autom. Constr.*, vol. 140, Aug. 2022, doi: 10.1016/j.autcon.2022.104389.
- 301 [13] T. H. Tran and N. D. Hoang, “Predicting algal appearance on mortar surface with ensembles of adaptive neuro
302 fuzzy models: a comparative study of ensemble strategies,” *Int. J. Mach. Learn. Cybern.*, vol. 10, no. 7, pp.
303 1687–1704, Jul. 2019, doi: 10.1007/s13042-018-0846-1.
- 304 [14] T. H. Tran and N. D. Hoang, “Estimation of algal colonization growth on mortar surface using a hybridization of
305 machine learning and metaheuristic optimization,” *Sadhana - Acad. Proc. Eng. Sci.*, vol. 42, no. 6, pp. 929–939,
306 Jun. 2017, doi: 10.1007/s12046-017-0652-6.
- 307 [15] A. L. C. Ottoni, R. M. De Amorim, M. S. Novo, and D. B. Costas, “Tuning of data augmentation hyperparameters
308 in deep learning to building construction image classification with small datasets,” *Int. J. Mach. Learn. Cybern.*,
309 vol. 14, no. 1, pp. 171–186, 2023, doi: 10.1007/s13042-022-01155-1.
- 310 [16] J. W. R. Chong *et al.*, “Microalgae identification: Future of image processing and digital algorithm,” *Bioresour.*
311 *Technol.*, vol. 369, no. November 2022, p. 128418, 2023, doi: 10.1016/j.biortech.2022.128418.
- 312 [17] “ASTM D4404-10. Standard test method for determination of pore volume and pore volume distribution of soil
313 and rock by mercury intrusion porosimetry. American Society for Testing and Materials.” American Society for
314 Testing and Materials, 2010.
- 315 [18] “UNI EN ISO 4287:2009. Geometrical Product Specifications (GPS) - Surface texture: Profile method - Terms,
316 definitions and surface texture parameters.” International Standards Organization, 2009.
- 317 [19] “ASTM D5589-09. Standard test method for determining the resistance of paint films and related coatings to
318 algal defacement. American Society for Testing and Materials.” 2009.
- 319 [20] “UNI EN ISO 12571:2013. Hygrothermal performance of building materials and products - Determination of
320 hygroscopic sorption properties.” 2013.
- 321 [21] R. Ferreira Maia, O. Bernard, A. Gonçalves, S. Bensalem, and F. Lopes, “Influence of temperature on *Chlorella*
322 *vulgaris* growth and mortality rates in a photobioreactor,” *Algal Res.*, vol. 18, pp. 352–359, 2016, doi:
323 10.1016/j.algal.2016.06.016.
- 324 [22] S. Lengsfeld and M. Krus, “Microorganism on façades – reasons, consequences and measures,” no. Venzmer,
325 pp. 0–7, 2001.
- 326 [23] “UNI EN 15886:2010. Conservation of cultural property - Test methods - Colour measurement of surfaces.” Ente
327 Nazionale Italiano di Unificazione (UNI), 2010.
- 328 [24] “UNI 11721:2018. Materiali lapidei - Metodi di prova – Misurazione preventiva della variazione colorimetrica di
329 superfici di pietra.” Ente Nazionale Italiano di Unificazione (UNI), 2018.
- 330 [25] S.-S. Baek *et al.*, “Identification and enumeration of cyanobacteria species using a deep neural network,” *Ecol.*

331 *Indic.*, vol. 115, p. 106395, Aug. 2020, doi: 10.1016/j.ecolind.2020.106395.
332

IN-PRESS VERSION